

Owl and Lizard: Patterns of Head Pose and Eye Pose in Driver Gaze Classification

Lex Fridman¹, Joonbum Lee¹, Bryan Reimer¹, and Trent Victor²

¹Massachusetts Institute of Technology (MIT)

²Chalmers University of Technology, SAFER

Abstract—Accurate, robust, inexpensive gaze tracking in the car can help keep a driver safe by facilitating the more effective study of how to improve (1) vehicle interfaces and (2) the design of future Advanced Driver Assistance Systems. In this paper, we estimate head pose and eye pose from monocular video using methods developed extensively in prior work and ask two new interesting questions. First, how much better can we classify driver gaze using head and eye pose versus just using head pose? Second, are there individual-specific gaze strategies that strongly correlate with how much gaze classification improves with the addition of eye pose information? We answer these questions by evaluating data drawn from an on-road study of 40 drivers. The main insight of the paper is conveyed through the analogy of an “owl” and “lizard” which describes the degree to which the eyes and the head move when shifting gaze. When the head moves a lot (“owl”), not much classification improvement is attained by estimating eye pose on top of head pose. On the other hand, when the head stays still and only the eyes move (“lizard”), classification accuracy increases significantly from adding in eye pose. We characterize how that accuracy varies between people, gaze strategies, and gaze regions.

Index Terms—Head pose estimation, pupil detection, gaze tracking, driver distraction, driver assistance systems, on-road study.

I. INTRODUCTION

The classification of driver visual attention allocation is an area of increasing relevance in the pursuit of accident reduction. The allocation of visual attention away from the road has been linked to accident risk [1], [2] and a drop in situational awareness as uncertainty in the environment increases [3]. Driver distraction is often construed as a key source of attention divergence from the roadway and the topic of numerous scientific studies and design guidelines [4], [5].

Furthermore, as the level of vehicle automation continues to increase through Advanced Driver Assistance Systems as well as other higher forms of automation, freeing available resources from the primary operational task, drivers are expected to be increasingly allowed to glance away from the roadway for greater periods. When the need arises to orient the driver to the roadway, different alerting strategies may be advantageous. Such work would suggest that a real-time estimation of drivers gaze could be coupled with an alerting system to enhance safety [6]. Gaze tracking from video in the driving context is a difficult problem due especially to

rapidly varying lighting conditions. Other challenges, common to other domains, include unpredictability of the environment, presence of eyeglasses or sunglasses occluding the eye, partial occlusion of the pupil due to squinting, vehicle vibration, image blur, poor video resolution, etc. We consider the challenging case of uncalibrated monocular video because it has been and continue to be the most commonly available form of video in driving datasets due to its low equipment and installation costs.

From the perspective of image processing, gaze estimation can be divided into two components: head pose estimation and eye pose estimation. Due to all the factors above, the latter is more difficult than the former. In fact, gaze classification performance can be good based on head pose alone [7], because it frequently correlates with eye pose, but not always. “Eye pose” and “head pose” are terms used throughout this paper to mean the relative orientation of the pupil in the eye socket and the relative orientation of facial features on the head, respectively. This use of “pose” is made broader in order to allow for the nonlinear modeling discussed in §IV-B.

In this paper, we seek to characterize when eye pose significantly contributes to gaze classification and when it does not. Specifically, we ask two questions:

- 1) **Contribution of Eye Pose:** How much better can we classify driver gaze using (a) head and eye pose together versus (b) using head pose alone.
- 2) **Classification of Different Gaze Strategies:** Are there individual-specific gaze strategies that strongly correlate with how much gaze classification improves with the addition of eye pose information?

These two questions are answered by analyzing data drawn from an on-road study of 40 drivers performing secondary tasks of varying complexity. The inter-person classification and gaze strategy variation is discussed using the analogy of an “owl” and “lizard” (introduced previously in [8], [9]) which describes the degree to which the eyes and the head move when shifting gaze. When the head moves a lot (“owl”), not much classification improvement is attained by estimating eye pose on top of head pose. On the other hand, when the head stays still and only the eyes move (“lizard”), classification accuracy increases significantly from adding in eye pose.

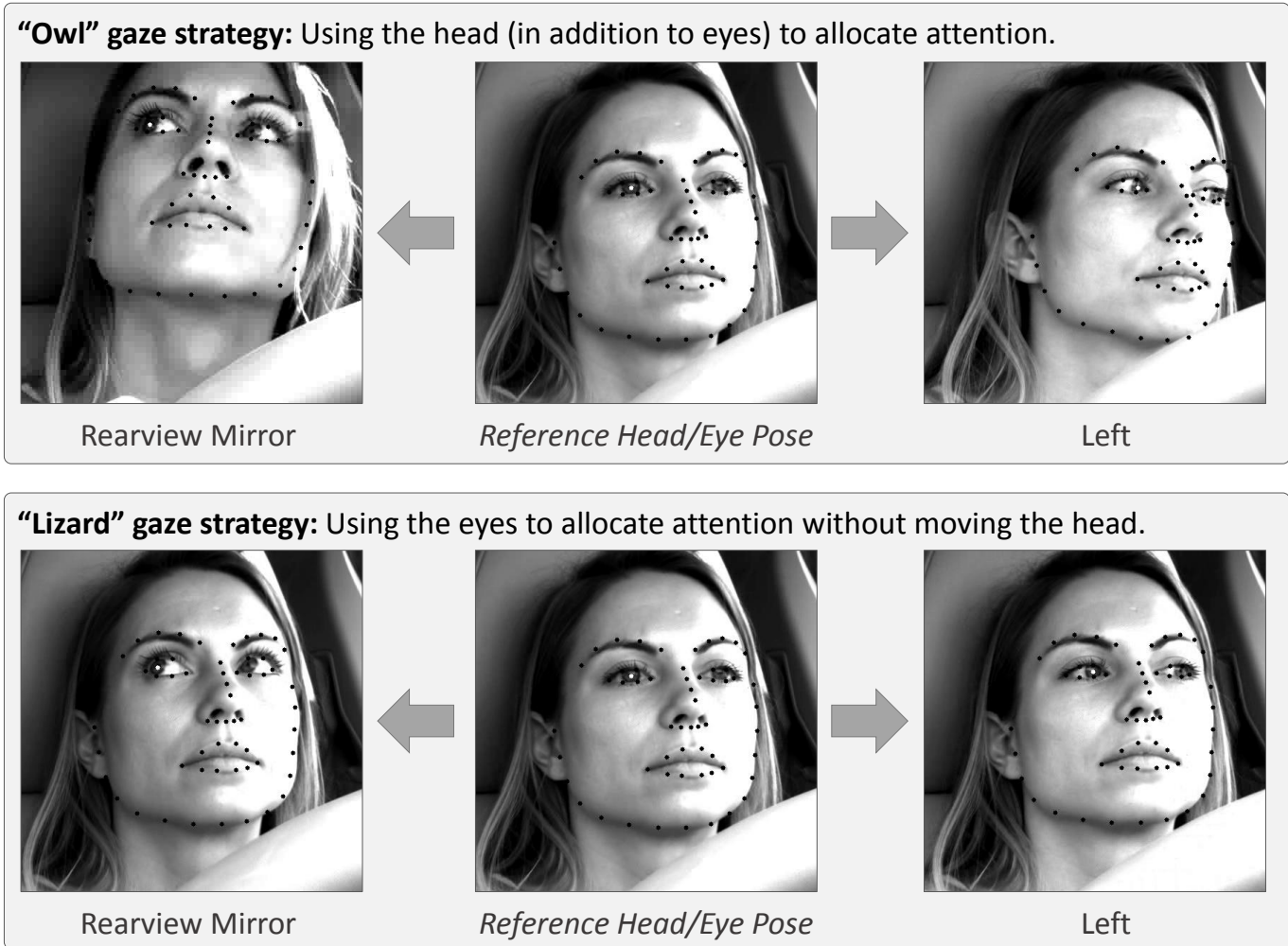


Fig. 1: Examples of gaze strategies that explain the “owl” and “lizard” analogy for head and eye pose. The “owl” gaze strategy involves primarily head movement, while the “lizard” gaze strategy involves primarily eye movement. The spectrum between these two is discussed in §V-B.

Examples of the two strategies are shown in Fig. 1. We propose an end-to-end driver gaze classification system based on monocular video and use it to explore the importance of eye pose for classification performance as we move along the spectrum of people from “owl” to “lizard”.

II. RELATED WORK

The problem of gaze tracking from monocular video has been investigated extensively across many domains [10], [11]. We build on this work to characterize the individual contribution of head movement and eye movement to gaze classification accuracy. The building blocks of our image processing pipeline are: face alignment, head pose estimation, and pupil detection. We apply cutting-edge algorithms from these fields to answer two questions posed by our work (see §I) on a large on-road driving dataset.

The algorithm in [12] uses an ensemble of regression trees

for super-real-time face alignment. Our face feature extraction algorithm draws upon this method as it is built on a decade of progress on the face alignment problem (see [12] for a detailed review of prior work). The key contribution of the algorithm is an iterative transform of the image to a normalized coordinate system based on the current estimate of the face shape. Also, to avoid the non-convex problem of initially matching a model of the shape to the image data, the assumption is made that the initial estimate of the shape can be found in a linear subspace.

Head pose estimation has a long history in computer vision. Murphy-Chutorian and Trivedi [13] describe 74 published and tested systems from the last two decades. Generally, each approach makes one of several assumptions that limit the general applicability of the system in driver gaze detection. These assumptions include: (1) the video is continuous, (2) initial pose of the subject is known, (3) there is a stereo vision system available, (4) the camera has frontal view of the face, (5) the head can only rotate on one axis, (6) the system only

has to work for one person. While the development of a set of assumptions is often necessary for the classification of a large number of possible poses, our approach skips the head pose estimation step (i.e. the computation of a vector in 3D space modeling the orientation of the head) and goes straight from the detection of a facial features to a classification of gaze to one of six glance regions. Prior work has shown that such a classification set is sufficient for the in-vehicle environment, even under rapidly shifting lighting conditions [7].

Pupil detection approaches have been extensively studied. Methods usually track corneal reflection, distinct pupil shape in combination with edge-detection, characteristic light intensity of the pupil, or a 3D model of the eye to derive an estimate of an individual’s pupil, iris, or eye position [14]. Our approach uses an adaptive CDF-based method [15] in conjunction with face alignment that significantly narrows the search space.

Studies of the correlation between head and eye movement have shown inter-person variation in the degree to which the head serves as a proxy for gaze [7], [9]. For example, a previous work tested drivers’ head movements while looking at the “road” and the “center stack” and found that: (1) drivers’ horizontal range of head movements varied (from 5 to 20 degrees) across individuals along with (2) their mean differences of horizontal head angles while looking at the two objects (from 0 to 10 degrees) [9]. This paper makes this variation more explicit by characterizing classification performance with and without eye pose information.

III. DATASET

Training and evaluation is carried out on a dataset of 40 subjects drawn from a larger driving study of 80 subjects that took place on a local interstate highway (see [16] for detailed experimental methods). For each subject, the collection of data was carried out in one of two vehicles: 2013 Chevrolet Equinox or Volvo XC60 (randomly assigned). The drivers performed a number of secondary tasks of varying difficulty including using the voice interface in the vehicle to enter addresses into the navigation system and using the voice interface as well as manual controls to select phone numbers from a stored phone list.

Both vehicles were instrumented with an array of sensors for assessing driver behavior. The sensor set included a camera positioned on the dashboard of each vehicle that was intended to capture the driver’s face for annotation of glance behavior. The cameras were positioned off-axis to the driver and in slightly different locations in the two vehicles (based upon features of the dashboard, etc.). As each driver positioned the seat (electronic in both vehicles) differently the relative position of the driver in relation to the camera varied somewhat by subject and across each driver over time (i.e., drivers move continuously in the seat, etc.). The camera was an Allied Vision Tech Guppy Pro F-125, capturing grayscale images at a resolution of 800x600 and speed of 30fps. The data

was double manually annotated for driver glances transitions during secondary task periods (at a resolution of sub-200ms) into one of 11 classes (road, center stack, instrument cluster, rearview mirror, left, right, left blindspot, right blindspot, passenger, uncodable, and other). As detailed in [16], any discrepancies between the two annotators were mediated by an arbitrator. This method of double annotation and mediation of driver gaze has been shown to produce very accurate annotations that can be effectively used as ground truth for supervised learning approaches [17].

Pruning Steps	Total Frames Remaining	Fraction of Original
0. Total Frames Annotated	1,351,864	100%
1. Frames with Faces Detected	1,073,380	79.4%
2. Frames with Pupils Detected	833,049	61.6%

TABLE I: Dataset statistics for the total number of video frames annotated, the number of frames where faces were detected, and the number of frames where pupil were detected. Each of these pruning steps are discussed in §IV.

In this paper, a broad random subset of data was drawn from the initial experiment and the “left” and “left blind spot” classes / “right”, “right blind spot”, “passenger” classes were collapsed respectively in to “left” and “right”. Periods that were labeled “uncodable” and “other” were excluded. Subject pruning was completed to ensure that every subject under consideration has sufficient training data for each of the six glance regions (road, center stack, instrument cluster, rearview mirror, left, and right). The threshold for “sufficient training” was that each subject had at least 120 frames of video (where pupils were detected) for each of the six gaze regions.

As shown in Table I, the resulting dataset contains 1,351,864 images each annotated as belonging to one of six glance regions. The algorithm described in §IV is used for face detection, face alignment, and pupil detection. The gaze classification approach requires a face and a pupil to be successfully detected in the image. The filtering procedure is discussed in detail in §IV. Therefore, in the evaluation we include only the images where a face and a pupil is detected. As the table shows, on average, a face is detected in 79.4% of images. 61.6% of images pass the full image processing pipeline where both a face and a pupil are detected.

IV. GAZE CLASSIFICATION PIPELINE

The steps in the gaze region classification pipeline are: (1) face detection, (2) face alignment, (3) pupil detection, (4) feature extraction and normalization, (5) classification, (6) decision pruning. If the system passes the first three steps, it will lead to a gaze region classification decision for every image fed into the pipeline. In step 6, that decision may be dropped if it falls below a confidence threshold (see §IV-E). The three face images in Fig. 2 are examples of the result achieved in the first four steps of the pipeline: going from a raw video frame

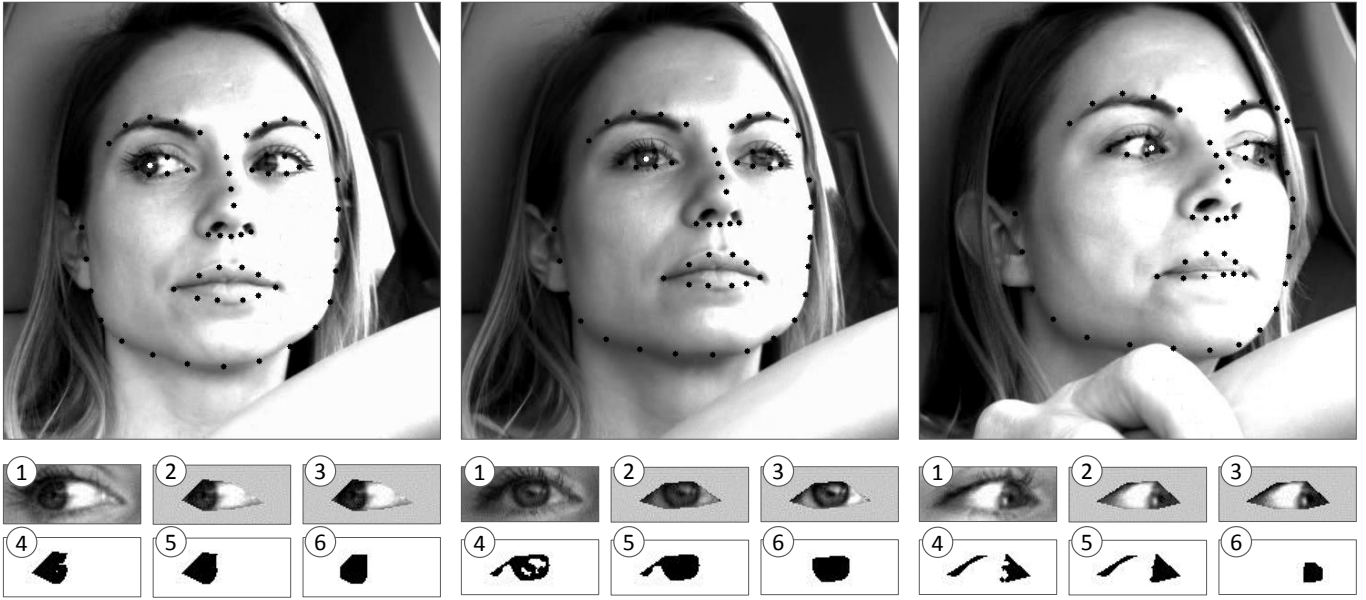


Fig. 2: Three example images showing the results of the feature extraction and the intermediate steps of the pupil detection. The black dots designate facial landmarks and the single white dot designates the pupil position in the right eye. There are 58 facial landmarks shown with 10 inner-mouth landmarks removed in the visualization for the purpose of visual clarity. Below each of the three face images are 6 steps of the pupil detection described in §IV-C.

to extracted face features and pupil position. As mentioned in §I, the relative orientation of facial features serves as a proxy for “head pose” and the relative orientation of pupil position serves as a proxy for “eye pose”. We discuss each of the six steps in the pipeline in the following sections.

A. Face Detection

The environment inside the car is relatively controlled in that the camera position is fixed and the driver torso moves in a fairly contained space. Thus, a camera can be positioned such that the driver’s face is always fully or almost fully in the field of view. However, the lighting conditions are sometimes drastically variable (e.g. quickly passing under a bridge, reflection of the sun on the camera lens, etc.) and thus there are frequently cases where the intensity distribution of the image does not allow for successful detection of the face (i.e. false reject). Every detection step in the pipeline is tuned to have a low False Accept Rate (FAR). A false accept error early in the pipeline propagates and can result in drastically incorrect head pose and eye pose estimation. In the context of video-based driver gaze classification, a high False Reject Rate (FRR) is more acceptable than a high FAR.

The face detector in our pipeline uses a Histogram of Oriented Gradients (HOG) combined with a linear SVM classifier, an image pyramid, and sliding window detection scheme implemented in the DLIB C++ library [18]. The performance of this detector has lower FAR than the widely-used default Haar-feature-based face detector available in OpenCV [19] and thus is more appropriate for our application.

B. Face Alignment and Head Pose

Both face alignment and head pose estimation are extremely well studied problems in computer vision [13], [20]. We investigated several cutting edge methods from each domain, and chose the ones that worked best for monocular video with highly varying lighting conditions.

Face alignment in our pipeline is performed on a 68-point Multi-PIE facial landmark mark-up used in the iBUG 300-W dataset [21]. These landmarks include parts of the nose, upper edge of the eyebrows, outer and inner lips, jawline, and parts in and around the eye. The selected landmarks are shown as black dots in Fig. 2. The algorithm for aligning the 68-point shape to the image data uses a cascade of regressors as described in [12] and implemented in [18]. The two characteristics of this algorithm most important to driver gaze localization is: (1) it is robust to partial occlusion and self-occlusion and (2) its running-time is significantly faster than the 30 fps rate of incoming images.

Face alignment produces estimates for facial feature positions in the image. These features can be mapped directly to a gaze region using methods that fall under the Nonlinear Regression category defined in [13]. They can also be mapped to a 3d model of the head. The resulting 3D-2D point correspondence can be used to compute the orientation of the head. This is categorized under Geometric Methods in [13]. Then the yaw, pitch, and roll of the head can be used as features for a gaze region classifier. We implemented both methods and found the former (nonlinear classification) to be more robust to errors in

the face alignment and pupil detection steps of the pipeline. The geometric approach uses OpenCV's SolvePnP solution of the PnP problem [22]. The nonlinear classification approach is discussed further in §IV-E.

C. Pupil Detection

As described in §I, the problem of accurate pupil detection is more difficult than the problem of accurate face alignment, but both are not always robust to poor lighting conditions. Therefore, the secondary task of pupil detection is to flag errors in the face alignment step that preceded it. As Table I shows, the face is detected in 79.4% video frames but only 61.6% of the original frames pass the pupil detection step.

We use a CDF-based method [15] to extract the pupil from the image of the right eye, and adjust the extracted pupil blob using morphological operations of erosion and dilation. The six steps in this process are as follows:

- 1) Extract the right eye from the face image based on the right eye features computed as part of the face alignment step.
- 2) Remove all pixels that fall outside the boundaries of the polygon defined by the 6 eye features.
- 3) Rescale the intensity such that the 98-percentile intensity becomes 1.0 intensity and 2-percentile intensity becomes 0.0 intensity.
- 4) Define a CDF intensity threshold and convert the grayscale image to a binary image. Each pixel intensity above the threshold becomes 1, and otherwise becomes 0.
- 5) Perform an “opening” morphology transformation (described in [23]). This operation is useful for removing small holes in large blobs.
- 6) Perform a “closing” morphology transformation (described in [23]). This operation is useful for removing small objects and smoothing the shape of large blobs.

The above steps have three parameters: the CDF threshold, the opening window size, the closing window size. These parameters are dynamically optimized for each image over a discrete set of values in order to maximize the size of the largest resulting blobs under one constraint: the largest blob must be circle-shaped (i.e. have similar height and width). More specifically, each of the 3 parameters take on 3 values and using exhaustive search we find the set of parameter values that results in the largest circular blob.

The pupil detection process also includes pruning procedures based on whether the eye is sufficiently open and whether there is a possible error in the preceding face alignment step. These are:

- 1) An eye shape height that is less than 10% of its width is considered “closed” and is removed from the pipeline.

- 2) When a sufficiently large blob is not found in the eye region (less than 5 pixels in area), it is assumed that the face alignment did not properly localize the eye and the image is removed from the pipeline.

D. Feature Extraction and Normalization

The driver spends more than 90% of their time looking forward at the road and this fact was used in [7] to normalize the position of facial features relative to the average bounding box of the face associated with the “Road” gaze region. This required an initial 120 second period of automated calibration. In this paper, we remove the need for calibration and instead normalize the facial features based on the bounding box of the eyes and nose for the current frame only. Fig. 1 shows departure of the head and eyes away from their “reference” positions. The normalization step linearly transforms the facial landmarks such that the landmarks of the eyes and nose fit a unit square. After this transformation, the relative orientation of the facial landmarks becomes the feature vector for the gaze classification step. The bounding box of the eyes and nose was experimentally found to be the most robust normalizing region. This is due to the fact that the greatest noise in the face alignment step was associated with the features of the jawline, the eyebrows and the mouth. The position of the pupil is normalized to the bounding box of the eye rotated such that the two eye corners lie on a horizontal line.

E. Classification and Decision Pruning

Scikit-learn implementation of a random forest classifier [24] is used to generate a set of probabilities for each class from a single feature vector. The probabilities are computed as the mean predicted class probabilities of the trees in the forest. The class probability of a single tree is the fraction of samples of the same class in a leaf. A random forest classifier of depth 25 with an ensemble of 2,000 trees is used for all experiments in §V. The class with the highest probability is the one that the system assigns to the image as the “decision”. The ratio of the highest probability to the second highest probability is termed the “confidence” of the decision. A confidence of 1 is the minimum. There is no maximum. The effect of this threshold is explored in [7]. For the experiments in §V a confidence threshold of 10 is used, which means that any decisions with a confidence greater than 10 are accepted and the others are ignored. A random forest classifier was used because it achieved a much higher accuracy than k-nearest neighbors (KNN) and linear SVM classifiers. RBF-kernel SVM achieved a slightly higher accuracy but at the cost of over a 100-fold increase in training time.

V. RESULTS

A. Gaze Region Classification

We evaluate the gaze classification pipeline described in §IV on the dataset of 40 drivers described in §III. In all the

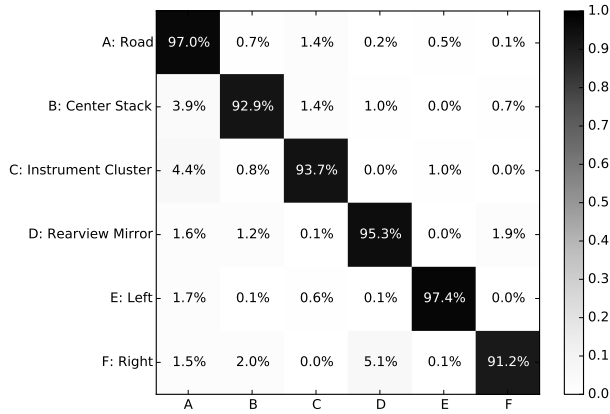


Fig. 3: Confusion matrix for the six-region classification problem for using both head pose and eye pose information. The overall accuracy is 94.6%. The confidence threshold is set to 10 resulting in an average confident decision rate of 2.3 times a second. When considering that only 61.6% of frames pass the face detection and pupil detection steps, the effective overall decision rate is 1.3 times a second.

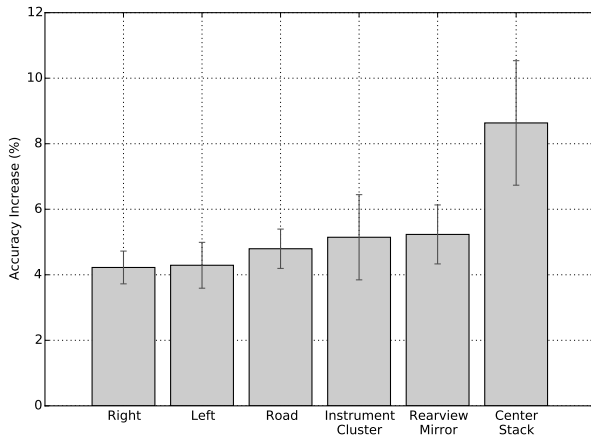


Fig. 4: Increase in accuracy per gaze region achieved by using eye pose in addition to head pose. The increase results in the confusion matrix show in Fig. 3.

experiments and discussions that follow, the key comparison is between classification performed using head pose alone and classification performed using head pose and eye pose together. The classification problem has six classes, one for each of the six gaze regions: (1) road, (2) center stack, (3) instrument cluster, (4) rearview mirror, (5) left, and (6) right.

The pipeline starts at an annotated frame from the raw video. As previously described, each frame is double annotated and mediated ensuring that the gaze region annotations can reliably serve as ground truth for the cross validation training and testing. There are a total of 1,351,864 annotated images. As show in Table I, 833,049 of those images pass through the face detection, face alignment, and pupil detection steps of the

pipeline. As discussed in §IV-E, we further reduce this number during testing by only considering decisions with a confidence above the confidence threshold of 10. On average, only 7.1% of all decisions are deemed confident in this way, resulting in a decision rate of 2.3 Hz. This selection is distributed evenly through time among cases where a face is successfully detected. If we consider the fraction of original raw video frames that lead to a confident gaze classification decision, then the overall effective decision rate is 1.3 Hz.

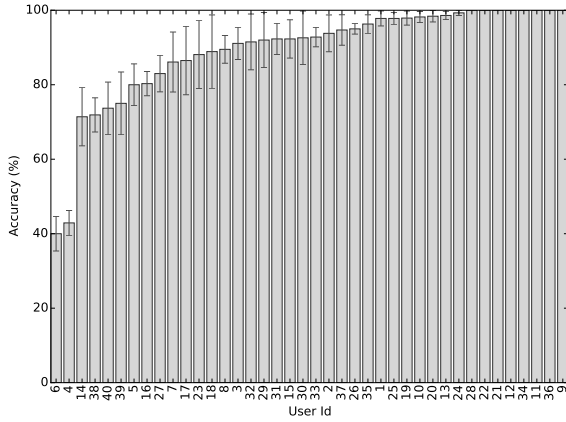
All of the plots in this sections share the same experiment setup. For each user, we train the 6-class classifier on all 39 others users. The training data for each of the 6 classes is balanced by random sub-sampling [25]. The testing is performed on the data for the one user by balancing the classes through super-sampling. This helps ensure that the per-class accuracy is not skewed by the greater representation of “Road” versus the other five classes in the dataset. The process is repeated 100 times for each of the 40 users. The plots with errorbars indicate the standard deviation of accuracy among the 100 runs for each user.

Fig. 3 shows the confusion matrix for classification using both head pose and eye pose. The overall accuracy achieved is 94.6%. Most of the errors in classification are in incorrectly labeling an image as “Road” when it is one of the other 5 gaze regions. Fig. 4 compares the accuracy in this confusion matrix with that achieved by a system that only uses head pose information. The overall accuracy achieved by such a system is 89.2%. One of the questions posed by this paper is: how much to we gain by considering eye pose on top of head pose? The answer in our final optimized system is 5.4% accuracy. As Fig. 4 shows, the biggest gain of 8.7% is achieved for the center stack region. This can be interpreted to mean that people are more likely to use only their eyes when glancing down to the center stack or that the head pose associated with the center stack is similar to the head pose of other gaze regions like “Road”, “Instrument Cluster”, and “Rearview Mirror” as Fig. 3 suggests.

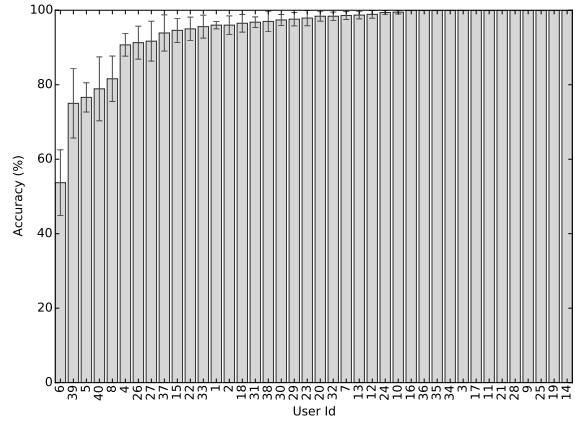
B. User-Specific Classification and Gaze Strategies

As shown in §V-A, adding in eye pose to head pose increases gaze classification accuracy by 5.4%. But that doesn’t tell the full story because some user-trained classifiers benefit more from eye pose than others. Fig. 5 shows the variation in accuracy among users before and after adding in eye pose to the classification feature set. For many users, 100% accuracy is achieved, while for many other accuracy drops to below 80% and even to as low as 40%.

Using the Pearson correlation coefficient as a guide, we programmatically explored over a million pairs of variables in search of an answer to the question of what explains this difference in classification performance between users. Some variables correlate with per-region accuracy but not overall. For example, average magnitude of off-center head movement

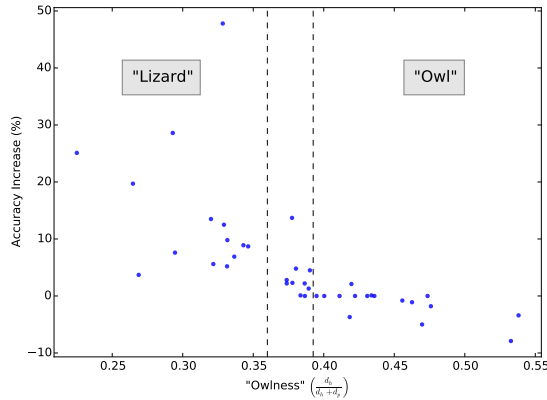


(a) Head pose alone. Average accuracy: 89.2%

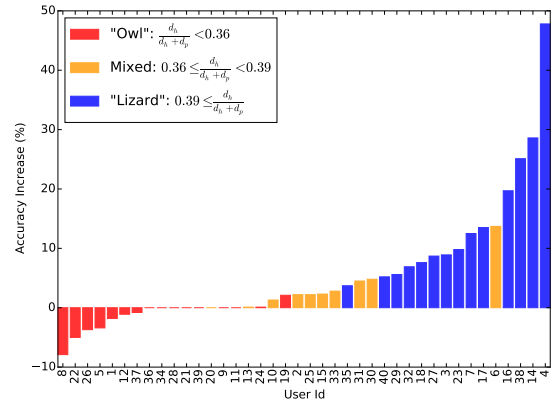


(b) Head pose and eye pose. Average accuracy: 94.6%

Fig. 5: Per-user accuracy in increasing order for confidence threshold of 10 and resulting decision rate of 2.31 times a second. The difference between the two is explored further in Fig. 6b.



(a) Increase in per-user accuracy versus the “owlness” metric which measures the fraction of the attention shift that is due to head movement versus eye movement. There are 40 points on this plot and each represents the average increase in accuracy achieved and the average measure of “owlness” for the user.



(b) Increase in per-user accuracy partitioned by two threshold values in the “owlness” metric. The users with the high “owlness” measures, see zero or less improvement from adding in eye pose. The users with the low “owlness” measures, see positive improvement from adding in eye pose.

Fig. 6: The “owlness” metric and its correlation with the increase in per-user accuracy from the first histogram plot to the second one in Fig. 5.

and pupil movement are good predictors of classification accuracy for the “Right” region with head pose alone and with head and eye pose together, respectively. We were not able to find a measure of an individual that correlated highly with overall classification accuracy, but there are a few variables that correlate with the increase in accuracy achieved by adding in eye pose. The most interesting and intuitive one is a metric we refer to as “owlness”. It is defined as:

$$M = \frac{d_h}{d_h + d_p} \quad (1)$$

where d_h and d_p are the distance of the nose tip and right pupil, respectively, from their average position in the back-

ground model. Due to the normalization of the features both distances are in the range $[0, \sqrt{2}]$. An M value of 0 means that a shift in gaze involves only the eyes (“lizard”). An M value of 1 means that a shift in gaze involves only the head (“owl”).

Fig. 6a shows the relationship between the “owlness” metric and the per-user increase in accuracy achieved. The measure of “owlness” for each user is computed by averaging the result of (1) for each image that passes the face detection and pupil detection steps in the pipeline. We partition users into three groups: “owl”, “lizard”, and “mixed” based on the value of M . Fig. 6b shows how effectively these partitions separate the users who gain classification accuracy from eye pose and those who do not. In this figure, the “owls” see no effect or

a decrease in accuracy, while the “lizards” see a significant increase in accuracy.

VI. CONCLUSION

This paper investigates the contribution of head pose and eye pose to gaze classification accuracy for different gaze strategies. We answer two questions: (1) how much does eye pose contribute and (2) how can the inter-user accuracy variation be explained? For the former, we show that eye pose adds a 5.4% increase in average accuracy (from 89.2% to 94.6%) with an effective average rate of 1.3 decisions per second. For the latter, we propose an “owlness” metric that decomposes gaze into head movement and eye movement and computes the relative magnitude of each. This metric is used to explain the inter-person variation in impact of eye pose on gaze classification accuracy.

ACKNOWLEDGMENT

Support for this work was provided by the Santos Family Foundation, the New England University Transportation Center, and the Toyota Class Action Settlement Safety Research and Education Program. The views and conclusions being expressed are those of the authors, and have not been sponsored, approved, or endorsed by Toyota or plaintiffs class counsel. Data was drawn from studies supported by the Insurance Institute for Highway Safety (IIHS).

REFERENCES

- [1] S. G. Klauer, T. A. Dingus, V. L. Neale, J. D. Sudweeks, and D. J. Ramsey, “The impact of driver inattention on near-crash/crash risk: An analysis using the 100-car naturalistic driving study data,” National Highway Traffic Safety Administration, Tech. Rep., 2006.
- [2] Y. Liang, J. D. Lee, and L. Yekhshatyan, “How dangerous is looking away from the road? algorithms predict crash risk from glance patterns in naturalistic driving,” *Human Factors: The Journal of the Human Factors and Ergonomics Society*, vol. 54, no. 6, pp. 1104–1116, 2012.
- [3] J. W. Senders, A. Kristofferson, W. Levison, C. Dietrich, and J. Ward, “The attentional demand of automobile driving,” *Highway research record*, no. 195, 1967.
- [4] N. H. T. S. Administration *et al.*, “Visual-manual nhtsa driver distraction guidelines for in-vehicle electronic devices,” *Washington, DC: National Highway Traffic Safety Administration (NHTSA), Department of Transportation (DOT)*, 2012.
- [5] D. F.-T. W. Group *et al.*, “Statement of principles, criteria and verification procedures on driver interactions with advanced in-vehicle information and communication systems,” *Alliance of Automotive Manufacturers*, 2006.
- [6] J. F. Coughlin, B. Reimer, and B. Mehler, “Monitoring, managing, and motivating driver safety and well-being,” *IEEE Pervasive Computing*, vol. 10, no. 3, 2011.
- [7] L. Fridman, P. Langhans, J. Lee, and B. Reimer, “Driver gaze estimation without using eye movement,” *IEEE Intelligent Systems*, 2016.
- [8] T. Victor, M. Dozza, J. Bärgrman, C.-N. Boda, J. Engström, and G. Markkula, *Analysis of Naturalistic Driving Study Data: Safer Glances, Driver Inattention, and Crash Risk*, 2014.
- [9] J. Lee, M. Muñoz, L. Fridman, T. Victor, B. Reimer, and B. Mehler, “Investigating drivers’ head and glance correspondence,” Submitted, 2016.
- [10] R. P. Gaur and K. N. Jariwala, “A survey on methods and models of eye tracking, head pose and gaze estimation,” in *Journal of Emerging Technologies and Innovative Research*, vol. 1, no. 5 (October-2014). JETIR, 2014.
- [11] M. Sireesha, P. Vijaya, and K. Chellamma, “A survey on gaze estimation techniques,” in *Proceedings of International Conference on VLSI, Communication, Advanced Devices, Signals & Systems and Networking (VCASAN-2013)*. Springer, 2013, pp. 353–361.
- [12] V. Kazemi and J. Sullivan, “One millisecond face alignment with an ensemble of regression trees,” in *Computer Vision and Pattern Recognition (CVPR), 2014 IEEE Conference on*. IEEE, 2014, pp. 1867–1874.
- [13] E. Murphy-Chutorian and M. M. Trivedi, “Head pose estimation in computer vision: A survey,” *Pattern Analysis and Machine Intelligence, IEEE Transactions on*, vol. 31, no. 4, pp. 607–626, 2009.
- [14] A. Al-Rahayfeh and M. Faezipour, “Eye tracking and head movement detection: A state-of-art survey,” *Translational Engineering in Health and Medicine, IEEE Journal of*, vol. 1, pp. 2 100 212–2 100 212, 2013.
- [15] M. Asadifard and J. Shanbezadeh, “Automatic adaptive center of pupil detection using face detection and cdf analysis,” in *Proceedings of the International MultiConference of Engineers and Computer Scientists*, vol. 1, 2010, p. 3.
- [16] B. Mehler, D. Kidd, B. Reimer, I. Reagan, J. Dobres, and A. McCartt, “Multi-modal assessment of on-road demand of voice and manual phone calling and voice navigation entry across two embedded vehicle systems,” *Ergonomics*, 2015.
- [17] D. Smith, J. Chang, R. Glassco, J. Foley, and D. Cohen, “Methodology for capturing driver eye glance behavior during in-vehicle secondary tasks,” *Transportation Research Record: Journal of the Transportation Research Board*, no. 1937, pp. 61–65, 2005.
- [18] D. E. King, “Dlib-ml: A machine learning toolkit,” *Journal of Machine Learning Research*, vol. 10, pp. 1755–1758, 2009.
- [19] R. Lienhart and J. Maydt, “An extended set of haar-like features for rapid object detection,” in *Image Processing. 2002. Proceedings. 2002 International Conference on*, vol. 1. IEEE, 2002, pp. I–900.
- [20] A. Wagner, J. Wright, A. Ganesh, Z. Zhou, H. Mobahi, and Y. Ma, “Toward a practical face recognition system: Robust alignment and illumination by sparse representation,” *Pattern Analysis and Machine Intelligence, IEEE Transactions on*, vol. 34, no. 2, pp. 372–386, 2012.
- [21] C. Sagonas, G. Tzimiropoulos, S. Zafeiriou, and M. Pantic, “300 faces in-the-wild challenge: The first facial landmark localization challenge,” in *Computer Vision Workshops (ICCVW), 2013 IEEE International Conference on*. IEEE, 2013, pp. 397–403.
- [22] G. Schweighofer and A. Pinz, “Globally optimal o (n) solution to the pnp problem for general camera models,” in *BMVC*, 2008, pp. 1–10.
- [23] G. Bradski and A. Kaehler, *Learning OpenCV: Computer vision with the OpenCV library*. O’Reilly Media, Inc., 2008.
- [24] F. Pedregosa, G. Varoquaux, A. Gramfort, V. Michel, B. Thirion, O. Grisel, M. Blondel, P. Prettenhofer, R. Weiss, V. Dubourg, J. Vanderplas, A. Passos, D. Cournapeau, M. Brucher, M. Perrot, and E. Duchesnay, “Scikit-learn: Machine learning in Python,” *Journal of Machine Learning Research*, vol. 12, pp. 2825–2830, 2011.
- [25] G. E. Batista, R. C. Prati, and M. C. Monard, “A study of the behavior of several methods for balancing machine learning training data,” *ACM Sigkdd Explorations Newsletter*, vol. 6, no. 1, pp. 20–29, 2004.